Reactions of 2-Propanol with Cu^+ in the Gas Phase: A Density Functional Theory Study

Mu-Jeng Cheng[†] and Ching-Han Hu*

Department of Chemistry, National Changhua University of Education, Changhua 500, Taiwan

Chen-Sheng Yeh

Department of Chemistry, National Chen Kung University, Tainan 701, Taiwan

Received: May 7, 2002; In Final Form: August 13, 2002

The gas phase reactions between Cu^+ and 2-propanol have been investigated using density functional theory at the B3LYP/6-311+G(d) and B3LYP/6-311++G(d,p) levels of theories. Seven reaction pathways have been studied. Of all reaction paths, the mechanism involving an electrophile-induced one step syn elimination of H_2O has the lowest energy barrier. Dehydration also occurs via the intermediate corresponding to C−O insertion of Cu^+. On the H_2 elimination channel, reaction begins with C−H insertion of Cu^+, followed by hydrogen migrations to form H_2−Cu^+−acetone or the H_2−Cu^+−2-propenol intermediates. Our results show that the reaction with copper cation insertion into the H−OCH$(CH_3)_2$ bond is unlikely, for its activation energy is 24.5 kcal/mol higher than those of the reactants (Cu^+ and 2-propanol). The mechanism involving C−C insertion of Cu^+ is also energetically unfavorable. The predicted potential energy surface of reaction and relative energies of the fragmentation products are consistent with available gas phase experiments.

1. Introduction

The importance of transition metal centers as catalysts for selective transformation of small molecules into useful chemical species has prompted extensive studies in the gas phase. Gas phase chemistry gives the opportunity of obtaining quantitative information regarding the dynamic, kinetic, and thermochemistry of elementary reactions in a controlled environment without disturbing factors.

Over the two past decades, considerable research, from both theoretical and experimental point of view, has been focused on understanding the ability in the gas phase of bare transition metal cations to activate bonds in small molecules.[1−20] Such studies provide thermochemistry detail as well as insight into the reaction mechanism. Experimentally, it has been shown that the reaction of the copper cation with 2-propanol leads to dehydration, dehydrogenation, or hydride abstraction in the gas phase.[1,21,22] Jones and Staley applied ion cyclotron resonance (ICR) spectrometry to study the gas phase chemistry of Cu^+ with alcohols.[21] Dehydration with the retention of H_2O or alkene and dehydrogenation were observed. It was proposed by the authors that an intermediate, which corresponds to O−H insertion of Cu^+, is involved in the dehydrogenation channel. The O−H-inserted intermediate, according to Staley and Jones, will lead to the elimination of CH_4. However, the mechanism was not supported by the experiment of Weil and Wilkins.[22]

Weil and Wilkins applied metal oxide (Cu_2O) in laser desorption/Fourier transform mass spectrometry (LD/FTMS) to study the reactions of Cu^+ with alcohols.[22] It was reported by this group that the most active channels are dehydration and dehydrogenation. The product percentage of dehydration with retention of propene is 7/3 times of that with retention of H_2O. A minor product is produced from the CuH + $Me_2C(OH)^+$ channel. Recently, Yeh et al. studied this reaction again by using a laser vaporization technique combined with a supersonic molecular beam expansion in a time-of-flight mass spectrometer.[1]

However, details for the reaction of Cu^+ and alcohol are yet to be clarified. In this paper, we study the reaction of copper cation with 2-propanol using density functional theory (DFT). The choice of 2-propanol is because of its richness in product channels. The potential energy surface (PES) of the reaction will benefit our knowledge on the mechanism of metal cation−alcohol reactions.

2. Computational Details

The theoretical treatment of the different systems included in this work was performed by using the B3LYP density functional approach in the Gaussian98 series of programs.[23] This B3LYP functional has been found to be quite reliable in describing the binding energies and PESs in metal cation−organic compound systems. The B3LYP approach is a hybrid method, which includes the Becke's three parameter nonlocal exchange potential[24] with the nonlocal correlation functional of Lee, Yang, and Parr.[25]

As a calibration of our approach, we performed a systematic study on the Cu^+−H_2O system. High-level ab initio theories including QCISD(T)[26] and CCSD(T)[27] were applied to study the binding energy of Cu^+−H_2O. These methods were used along with a list of basis sets, the largest being 6-311++G(3df,2p). The effects of electron correlation and basis functions on the accuracy of our computations are abstracted from the systematic analyses. Basis set superposition errors (BSSE) are accounted for using the counterpoise (CP) correction.[28]

The geometries of the different species under consideration were optimized using analytic gradients. The harmonic vibrational frequencies of the different stationary points of the PES

* To whom correspondence should be addressed. E-mail: chingkth@cc.ncue.edu.tw.

[†] Present address: Department of Chemistry, National Tsing Hua University, Hsinchu 300, Taiwan.

10.1021/jp0211335 CCC: $22.00
Published on Web 11/01/2002

TABLE 1: Predicted Binding Energies (D_e, in kcal/mol) of Cu^+-H_2O; D_0 Is Summarized in Parentheses

	MP4	QCISD	QCISD(T)	CCSD	CCSD(T)	B3LYP
			This Work[a]			
6-31G(d)	62.3 (60.1)	63.0 (60.8)	49.0 (46.8)	56.8 (54.6)	57.6 (55.4)	76.1 (74.4)
6-31+G(d)	45.5 (43.9)	43.5 (41.8)	39.3 (37.7)	41.1 (39.4)	42.1 (40.4)	44.3 (42.8)
6-31G(d,p)	62.0 (59.6)	62.6 (60.2)	48.8 (46.4)	56.5 (54.1)	57.2 (54.8)	76.5 (74.7)
6-31+G(d,p)	44.2 (42.6)	42.3 (40.7)	38.0 (36.4)	39.9 (38.3)	40.8 (39.2)	43.7 (42.4)
6-31++G(d,p)	44.3 (42.7)	42.3 (40.7)	38.1 (36.5)	39.9 (38.3)	40.8 (39.2)	43.9 (42.3)
6-311G(d)	44.3 (42.1)	44.3 (42.1)	39.6 (37.4)	41.9 (39.7)	42.1 (39.9)	53.3 (51.1)
6-311+G(d)	45.9 (43.9)	43.0 (41.1)	41.7 (39.8)	41.6 (39.6)	42.7 (40.7)	45.0 (43.0)
6-311G(d,p)	41.1 (39.2)	41.3 (39.1)	36.5 (34.6)	38.7 (36.9)	38.9 (37.0)	51.1 (49.1)
6-311+G(d,p)	41.0 (39.5)	38.4 (36.9)	37.1 (35.6)	37.0 (35.5)	37.9 (36.4)	41.9 (40.2)
6-311++G(d,p)	40.9 (39.5)	38.3 (36.9)	37.0 (35.6)	36.9 (35.5)	37.9 (36.4)	41.9 (40.2)
6-311+G(2df,2p)	41.4 (40.0)	38.0 (36.6)	37.5 (36.1)	36.8 (35.4)	38.0 (36.5)	41.0 (39.6)
6-311+G(3df,2p)	41.9 (40.4)	38.2 (36.7)	38.1 (36.6)	37.1 (35.6)	38.4 (36.9)	41.0 (39.7)
			Literature			
theory	38.2[b]				37.2[c]	40.8[c]
experiment	35 ± 3[d], 37.5 ± 1.9[e]					

[a] The G2 theory predicts D_0 of 33.6 kcal/mol from this work. [b] Ref 33. [c] Ref 32. [d] Ref 35. [e] Ref 36.

have been calculated at the same level of theory used for their optimization in order to identify the local minimum and the transition state (TS), as well as to estimate the corresponding zero-point vibrational energy (ZPVE). To identify which minima are connected by a given TS, we have performed intrinsic reaction coordinate (IRC) calculations at the B3LYP/6-31+G(d) level of theory.[29]

3. Results and Discussion

Cu^+-H_2O System. There have been extensive theoretical studies on the binding energy of Cu^+-H_2O.[30−34] The experimental measurement of the binding energy between Cu^+ and H_2O was reported to be 35 ± 3[35] and 37.5 ± 1.9[36] kcal/mol, respectively. Our computational results on the Cu^+-H_2O (C_{2v}) binding energy are summarized in Table 1. With the largest basis set (6-311++G(3df,2p)), B3LYP and the ab initio correlated methods converge to values that are in good agreement with the experimental observations. The 6-31G(d) basis provides poor predictions, and the results are significantly improved with the inclusion of diffuse functions on Cu (1s2p1d) and on O (1s1p). The diffuse functions on hydrogens do not make a noticeable difference. Energetics computed at the two largest basis sets, i.e., 6-311+G(2df,2p) and 6-311+G(3df,2p), are relatively close to those obtained using the 6-311+G(d,p) and 6-311++G(d,p) sets. It is noticed that in these two large basis sets, *g*-type polarization functions are included in Cu.

According to the data, the relatively small basis set 6-31+G(d) may be an economic choice for the computations of the 2-propanol−Cu^+ reactions. To understand the cause of the significant differences caused by basis functions, we computed the estimated BSSE using the CP correction scheme. The magnitude of CP corrections, from both the Cu^+ and the 2-propanol counterparts of the complex, is summarized in Table 2. It is seen that the CP corrections for the Cu^+ counterpart of the complex ($\Delta E_{CP}(Cu^+)$) are very large for basis sets without diffuse functions. On the basis of the experience, we have chosen two basis sets in our calculations on the PESs of Cu^+−2-propanol: 6-31+G(d) and 6-311++G(d,p). The 6-311++G(d,p) basis set is supposed to be capable of providing converged energetic predictions, while the comparison with the smaller 6-31+G(d) set should provide the possibility of using the much more economic approach in future studies.

Description of Reaction Paths Studied. On the PESs of Cu^+ and propanol reaction, a Cu^+−2-propanol complex (complex **1**) is formed first. During our attempts in the search of various possible reaction pathways, we located seven paths. We will briefly describe the mechanisms involved, while the detail of PESs will be discussed later in the text. The first path involves an electrophile-induced syn elimination of H_2O, forming complex **2** (H_2O-Cu^+-propene). The reaction is then followed by H_2O or propene dissociation (see Figure 1, path I). The second path (path II) begins with oxidation addition (C−O insertion) of **1**; the resulting complex **3** then rearranges via hydrogen shift to form complex **2**. The third path (path III, see Figure 2) results in H_2 elimination and hydride abstraction of Cu^+. The early intermediate **4** corresponds to that of a C−H insertion product; however, it adopts a triangular structure. The reaction then undergoes a relatively flat region on PES (**TS4-5**, **5**, and **TS5-6**) before forming complex **6**. From **6**, the H_2-eliminated precursor and the CuH + Me_2COH^+ fragments are produced. Path IV (Figure 3) coincides path III before complex **5**, after which the 1,4-H transfer leads to H_2-Cu^+-2-propenol (**8**). Complex **8** either dissociates into dehydrogenation products or rearranges into **7**. An alternative dehydrogenation mechanism is the direct, electrophile-assisted H_2 elimination (path V, Figure 4). Reaction paths VI (Figure 4) and VII (Figure 5) correspond to the O−H and C−C insertions of Cu^+, respectively. Detailed geometrical parameters optimized at the B3LYP/6-311++G(d,p) are shown in Figure 6.

TABLE 2: Magnitudes of BSSE Corrections Contributing to the Binding Energies (D_0, in kcal/mol) of Cu^+-H_2O; Results Are Obtained at the B3LYP Level of Theory

	D_0	$\Delta E_{CP}(Cu^+)$	$\Delta E_{CP}(H_2O)$	D_0(CP)
6-31G(d)	74.4	25.4	4.0	45.0
6-31+G(d)	42.8	0.7	1.7	40.4
6-31G(d,p)	74.7	25.8	4.2	44.7
6-31+G(d,p)	42.4	0.7	1.4	40.3
6-31++G(d,p)	42.3	0.7	1.4	40.2
6-311G(d)	51.1	8.9	1.9	40.3
6-311+G(d)	43.0	0.2	2.8	40.1
6-311G(d,p)	49.1	9.3	1.7	38.1
6-311+G(d,p)	40.2	0.2	1.3	38.8
6-311++G(d,p)	40.2	0.2	1.2	38.9
6-311+G(2df,2p)	39.6	0.2	0.3	39.1
6-311+G(3df,2p)	39.7	0.2	0.1	39.4

Cu^+-2-Propanol PES. The total energies, including ZPVE (in Hartree), and relative energies (in kcal/mol) of stationary points involved in the reactions (relative to **1**) are summarized in Table 3. In general, the relative energies computed at the B3LYP/6-31+G(d) level are close to those predicted using B3LYP/6-311++G(d,p). It is noted that the 6-31+G(d) set of Cu adopts the Pople split valence contraction.[37] In contrast, the

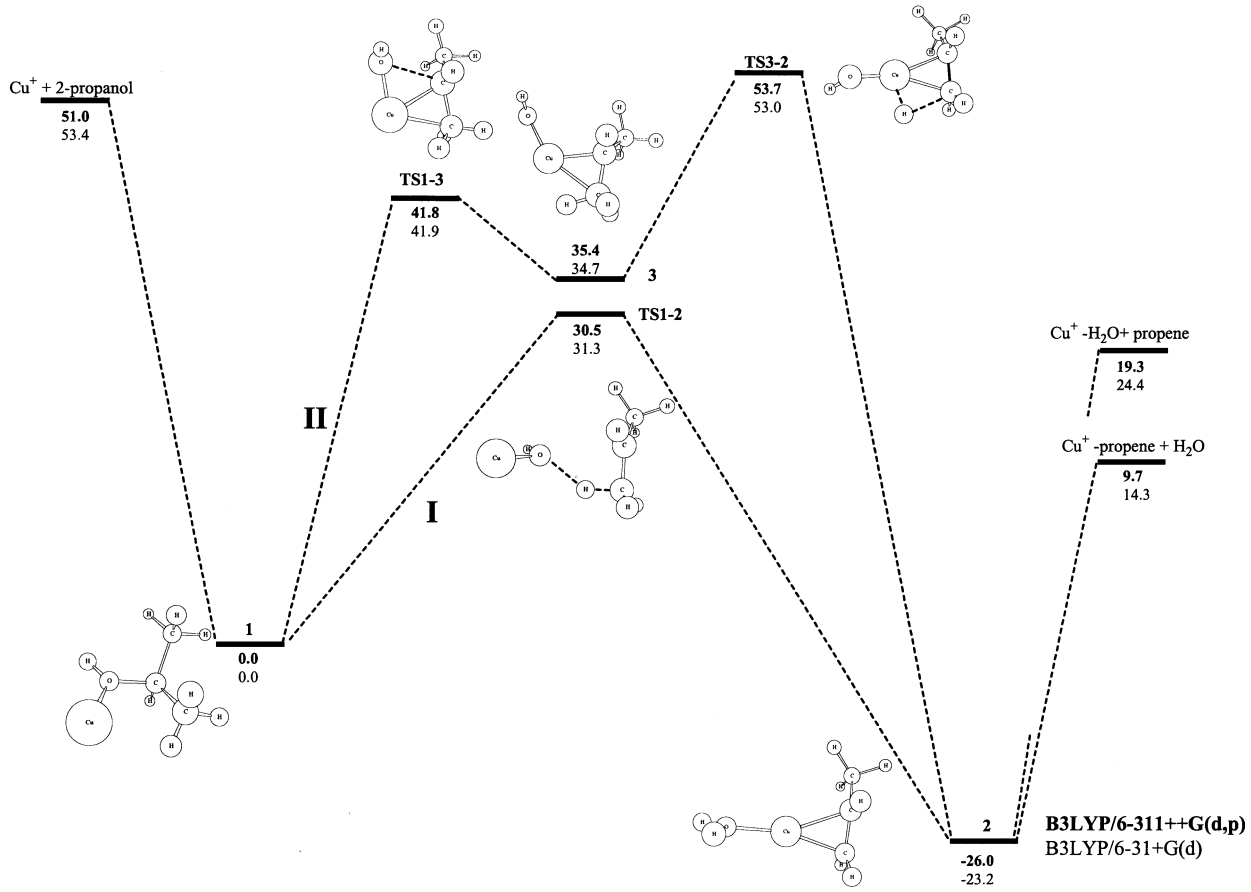

Figure 1. Potential energy diagram of the Cu^+-2-propanol reaction via elimination of H_2O (paths I and II). Energies (in kcal/mol) relative to **1** were obtained using the B3LYP/6-311++G(d,p) methods.

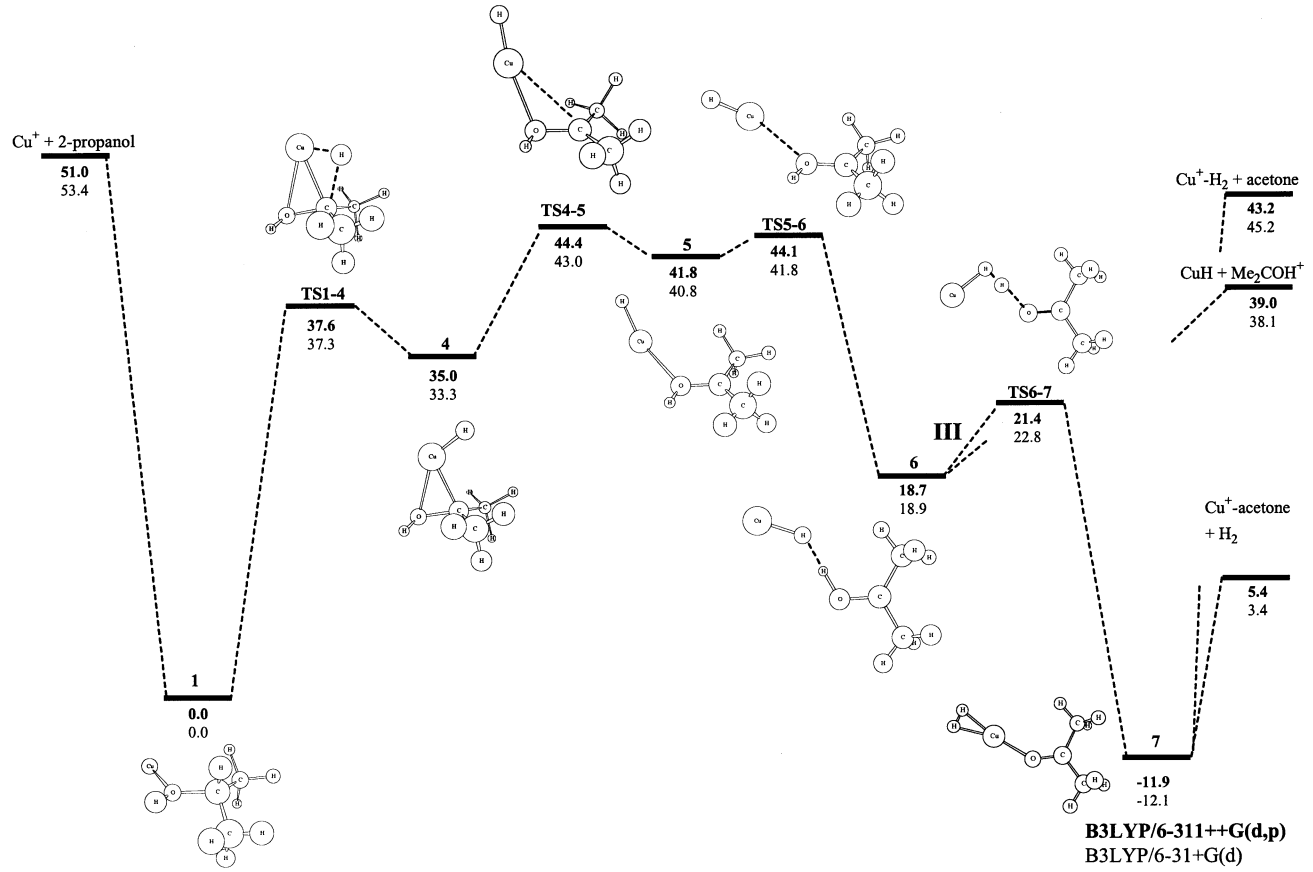

Figure 2. Potential energy diagram of the Cu^+-2-propanol reaction via elimination of H_2 (path III). Energy of **TS5-6** was obtained using single-point B3LYP/6-311++G(d,p)//B3LYP/6-31+G(d).

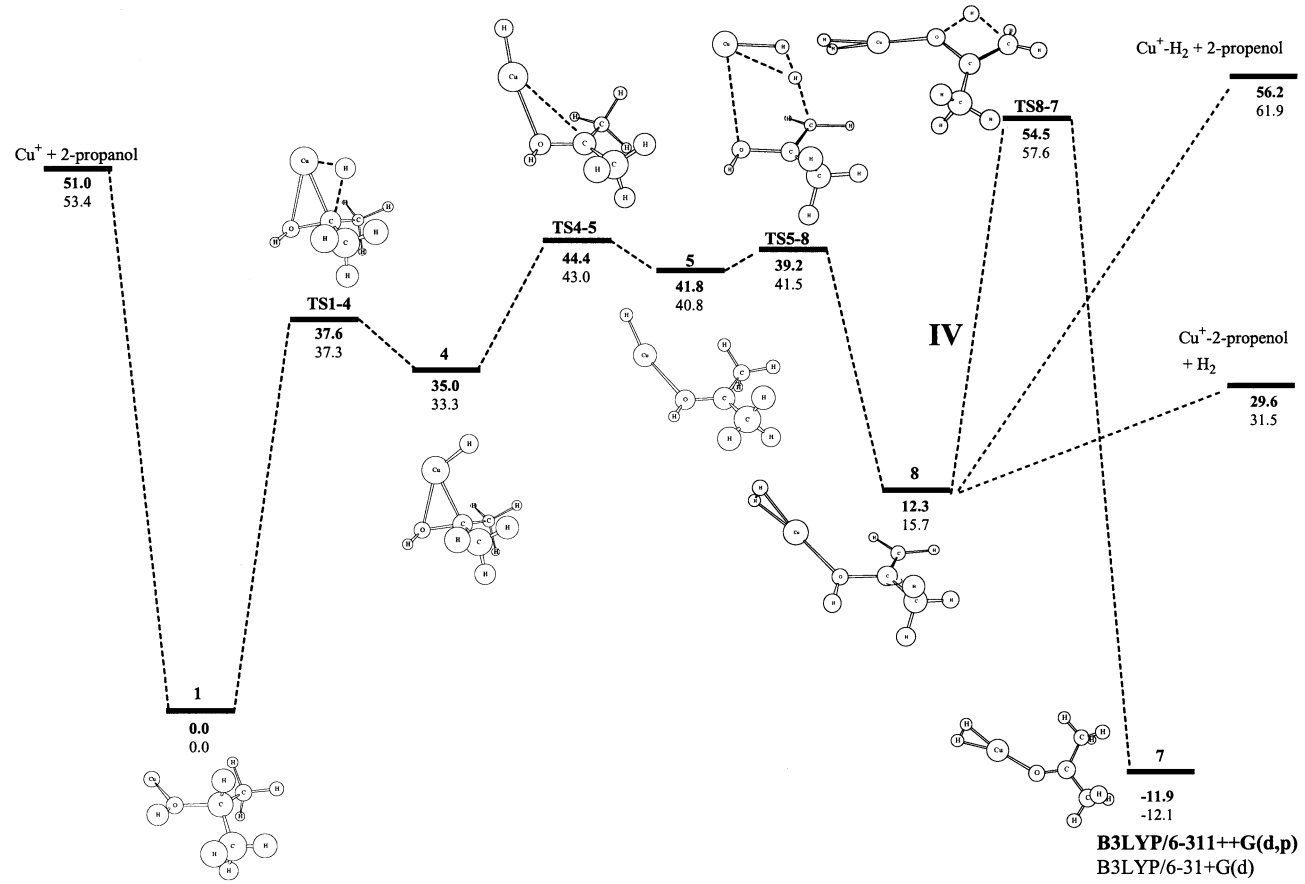

Figure 3. Potential energy diagram of the Cu^+-2-propanol reaction via elimination of H_2 (path IV).

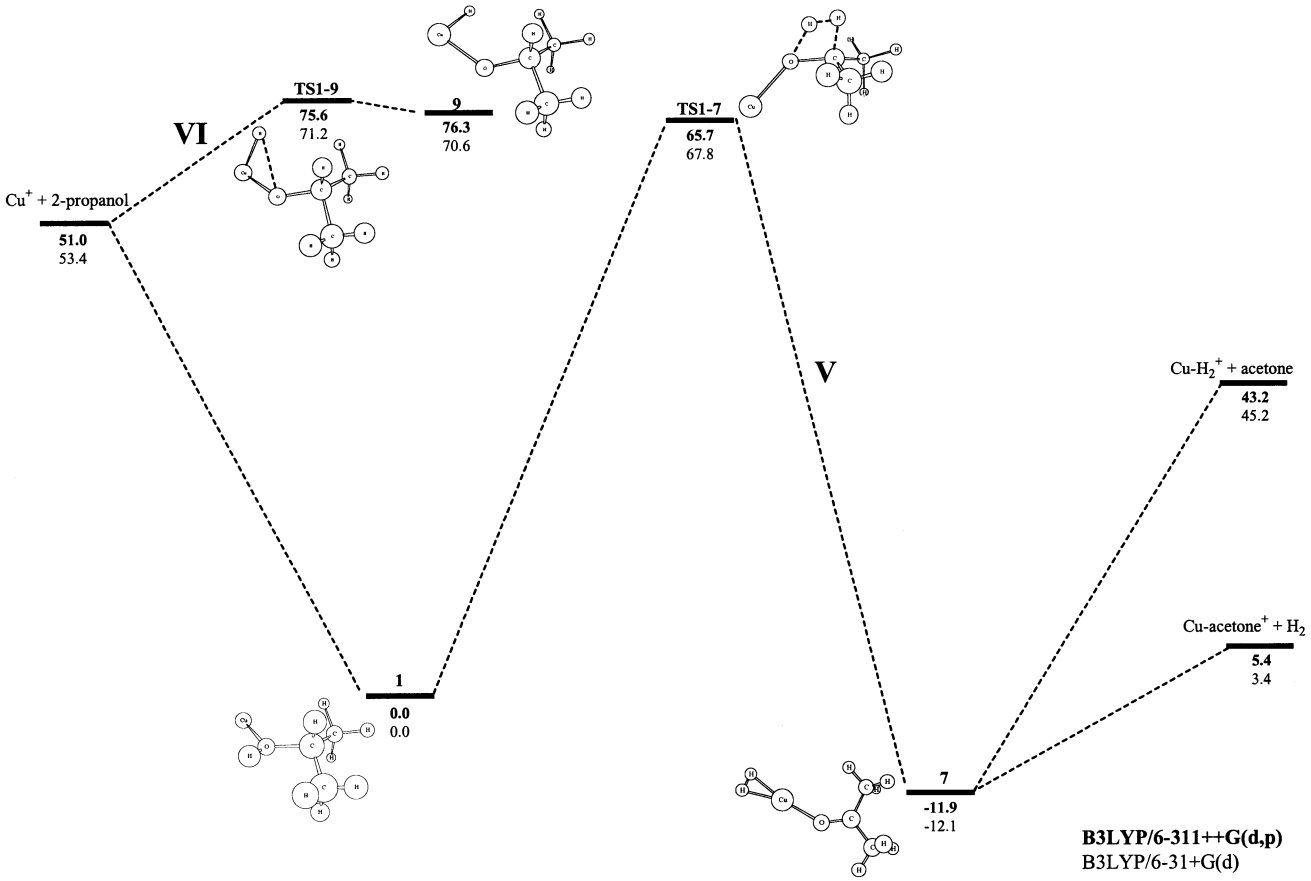

Figure 4. Potential energy diagrams of the Cu^+-2-propanol reaction via the direct, electrophile-assisted H_2 elimination (path V) and the O−H insertion (path VI). Energy of **9** was obtained using single-point B3LYP/6-311++G(d,p)//B3LYP/6-31+G(d).

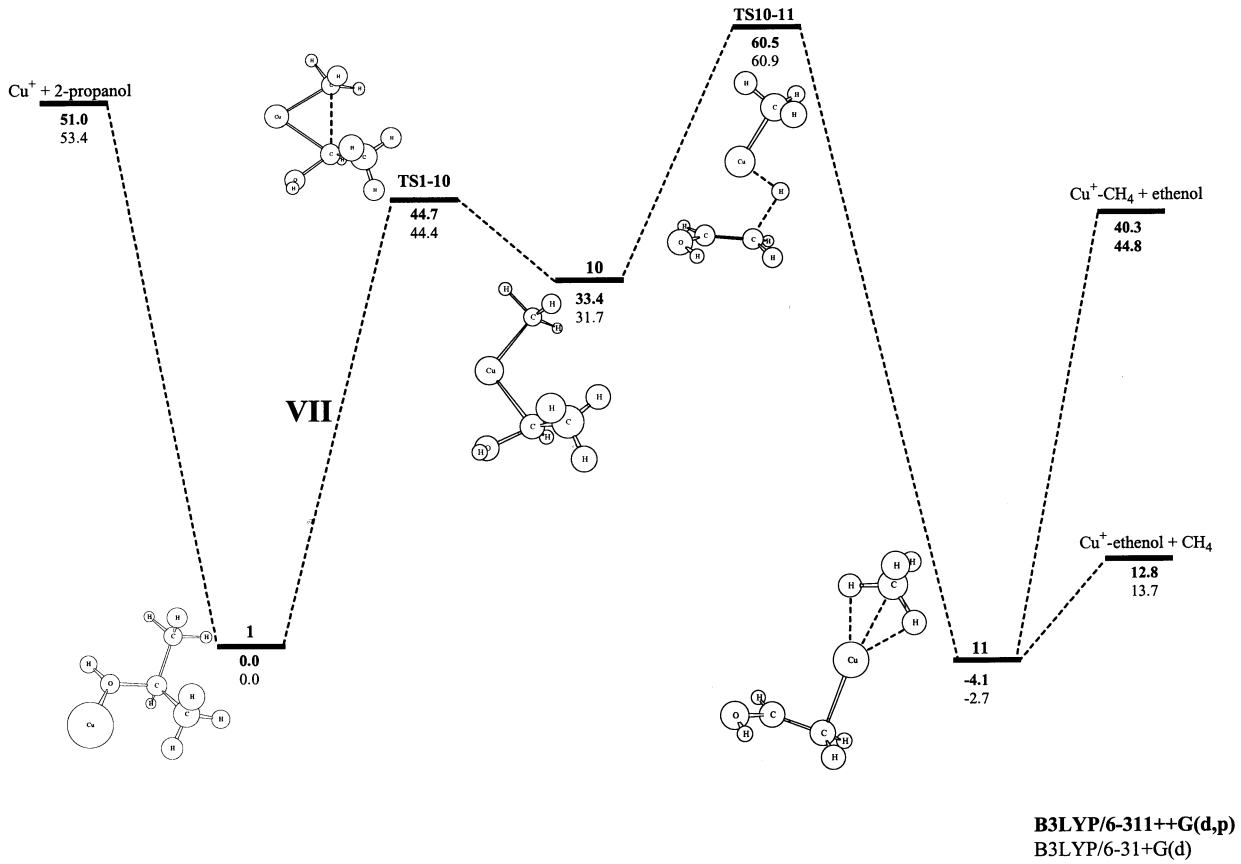

Figure 5. Potential energy diagrams of the Cu^+-2-propanol reaction via C−C insertion (path VII).

6-311++G(d,p) set of Cu corresponds to the Wachters−Hay's (14s9p5d/9s5p3d) basis set, using the same set of polarization and diffuse functions.[38] In the following discussions, we use the B3LYP/6-311++G(d,p) results.

As seen in Figure 1, the first step of the reactions of Cu^+ with 2-propanol is the formation of Cu^+-2-propanol (**1**). The binding energy of Cu^+-2-propanol is 51.0 kcal/mol with a Cu^+-O distance of 1.925 Å (see Figure 6). The predicted binding energy of Cu^+-2-propanol is 10.8 kcal/mol higher in energy than that predicted for Cu^+-H_2O, indicating the enhancement of the intrinsic basicity of the 2-propanol toward copper cation. Cu^+-2-propanol basically conserves the molecular structure of 2-propanol (Figure 6). The most noticeable differences are that the C−O bond distance is lengthened by 0.064 Å by complexation with Cu^+, while at the same time the C−C distances are slightly shorter. This implies a certain degree of charge redistribution within the 2-propanol subunit and leads to an activation of the C−O bond. The Cu−O−H−C fragment is close to planar (with a dihedral angle of 172.6°), which implies an ion−dipole interaction.[34]

For path I, the one step is the syn elimination of H_2O via hydrogen transfer through **TS1-2**. The activation barrier that connects the species **1** and **2** is 30.5 kcal/mol. This value is much lower than the barrier of 61.2 kcal/mol found for the dehydration of 2-propanol in the gas phase (at the B3LYP/6-311++G(d,p) level of theory). The one step reaction of **1** → **2** is exothermic (−26.0 kcal/mol) as compared to the exothermicity of 8.5 kcal/mol for 2-propanol in the gas phase. The geometry of **TS1-2** indicates that the TS is relatively late (C−O distance is 2.628 Å) as compared to that of the dehydration of 2-propanol in the gas phase, of which the C−O distance at the TS is 2.161 Å. Species **2** may eventually dissociate into either H_2O + Cu^+-propene or to propene + Cu^+-H_2O. Such a reaction path is in agreement with the mechanism proposed by Wilkins et al.[22]

In reaction path II, complex **1** forms the C−O insertion intermediate **3**, which lies higher in energy (35.4 kcal/mol) than the TS of the syn elimination (30.5 kcal/mol). The relative energy of the corresponding TS (**TS1-3**) lies 41.8 kcal/mol on the surface. Mulliken charge analyses of **1** and **3** indicate that the charge of copper atom decreases from 0.76 to 0.4, while the charge of C_2 (the iso-carbon) increases from −0.12 to 0.3 along the reaction path. This process characterizes an oxidative addition reaction. Complex **3** has a somewhat chelated structure where $Cu-C_2$ and $Cu-C_1$ bond distances are 1.984 and 2.177 Å, respectively (see Figure 6). The C_2-Cu-C_1 angle is 41.8°. From **3**, a further 1,2-hydrogen shift leads the reaction to the global minimum **2**, which dissociates into either H_2O + Cu^+-propene or propene + Cu^+-H_2O. Although the overall energy barrier of reaction path II was 23.2 kcal/mol higher in energy than that of path I, the mechanism is still feasible since the relative energy of **TS3-2** is comparable to that of free Cu^+ and 2-propanol. A dynamics study would benefit our understanding on the relative importance of the two paths.

In the dehydrogenation (path III) mechanism (Figure 2), complex **1** undergoes C−H insertion to form species **4** (35.0 kcal/mol) via a TS species **TS1-4** (37.6 kcal/mol). According to Mulliken charge, the reaction also characterizes an oxidative addition. The intermediate **5** is formed from **4** by breaking the C−O bond via **TS4-5**. The overall structure of **TS4-5** is close to that of the ion molecular **5**. The magnitude of imaginary frequency in **TS4-5** is very small (82 cm^{-1}). Mulliken charge analysis shows that the charge of C_2 in **5** is 0.83, and the geometry near C_2 is close to planar. The data indicate that **5** bears its positive charge mostly on C_2. A small activation energy leads to **TS5-6**, which connects species **5** and **6**. **TS5-6** is located

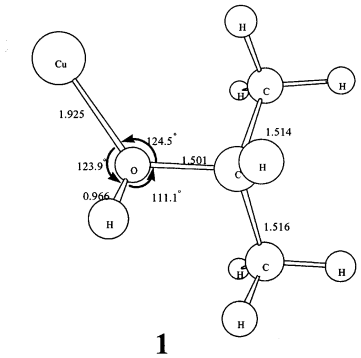

1

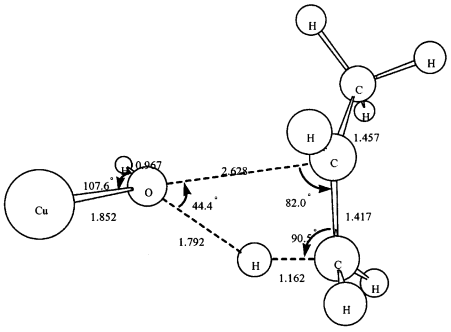

TS1-2

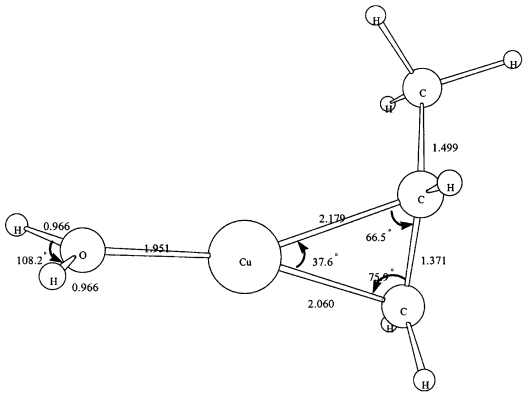

2

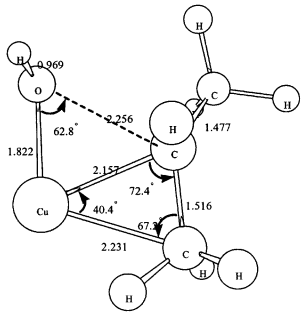

TS1-3

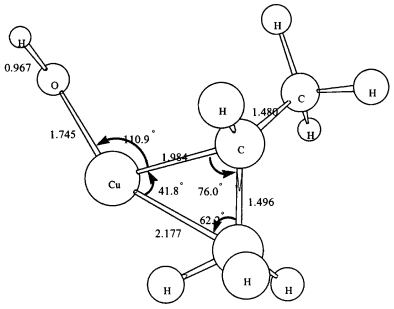

3

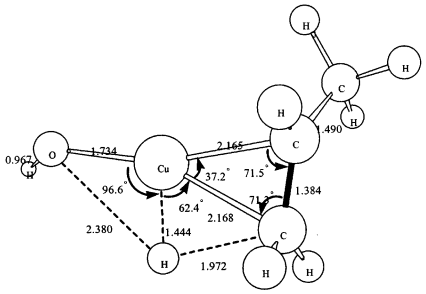

TS3-2

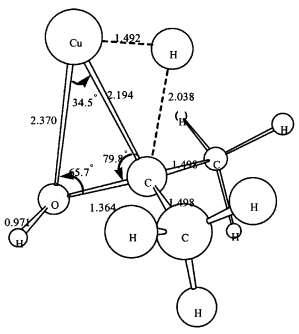

TS1-4

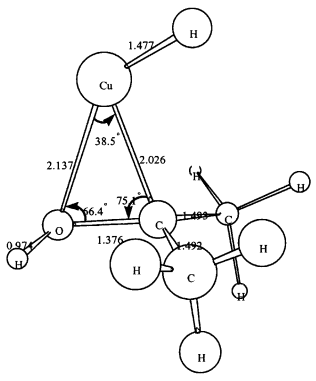

4

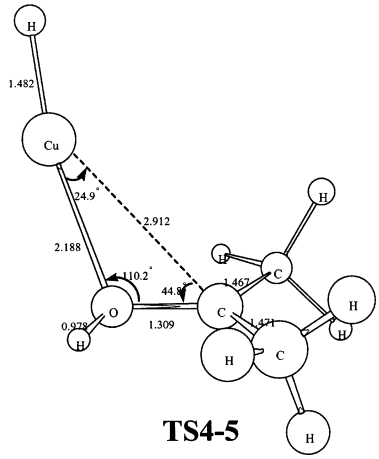

TS4-5

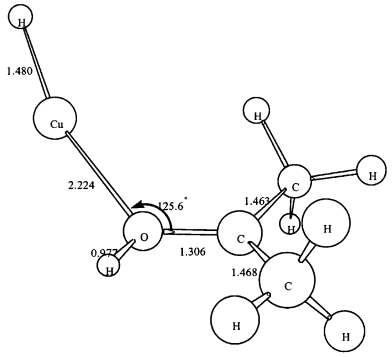

5

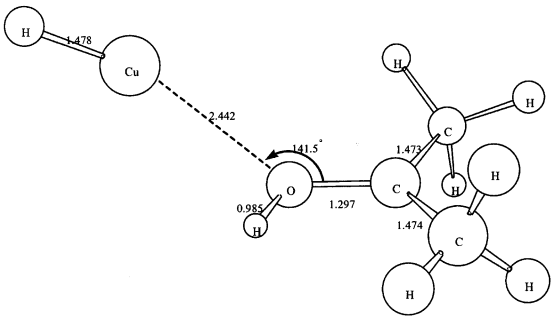

TS5-6

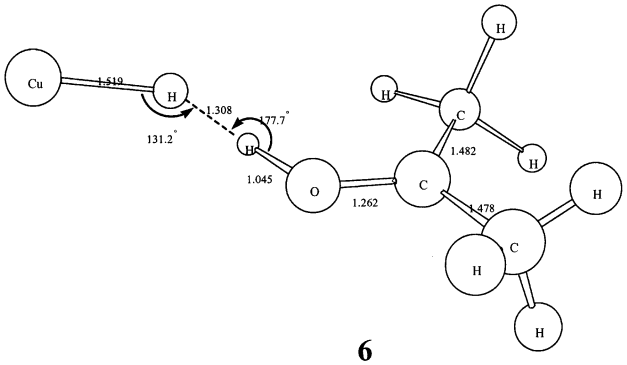

6

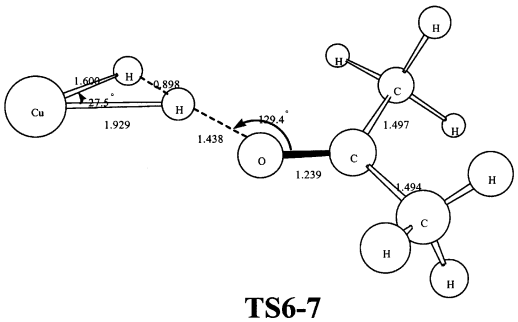

TS6-7

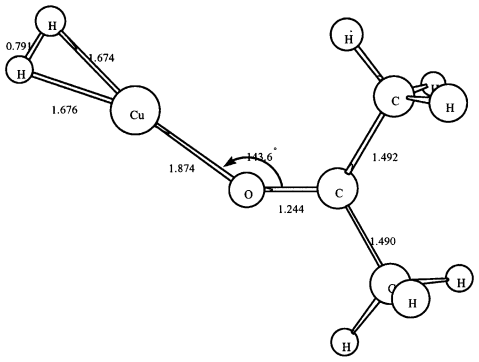

7

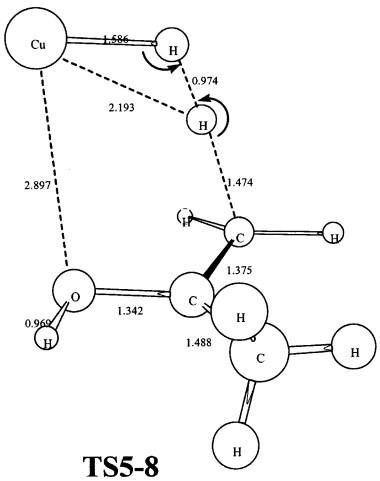

TS5-8

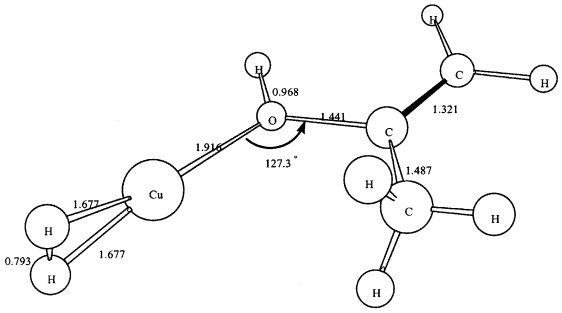

8

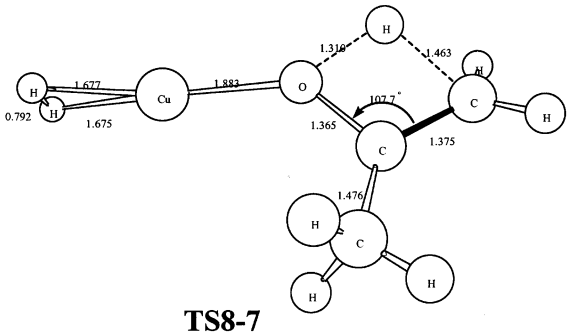

TS8-7

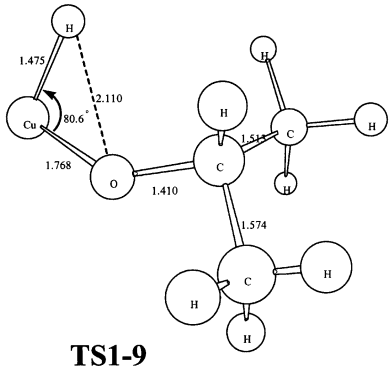

TS1-9

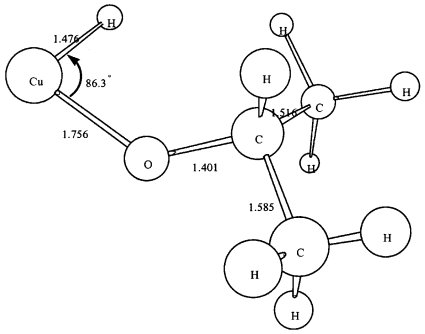

9

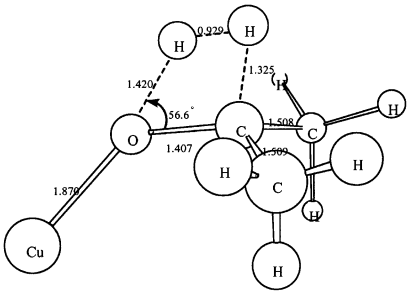

TS1-7

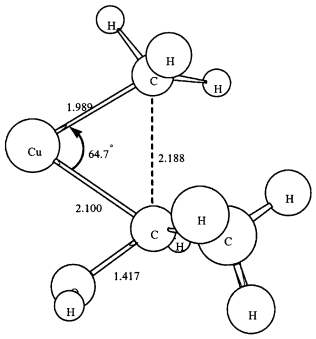

TS1-10

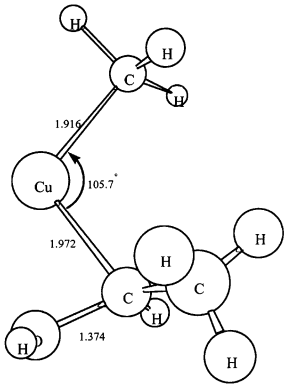

10

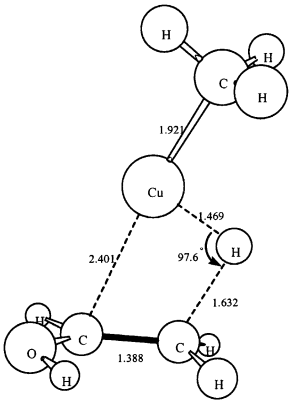

TS10-11

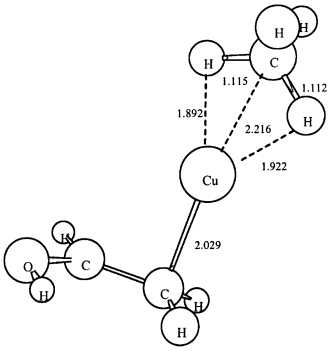

11

Figure 6. Schematic illustration of the optimized structures of species in the 2-propanol−Cu^+ reaction. Geometries were optimized at the B3LYP/6-311++G(d,p) level, exceptions are **TS5-6** and **9**, which were optimized using B3LYP/6-31+G(d).

TABLE 3: Total Energies and Relative Energies (kcal/mol) of the Stationary Points at the B3LYP/6-31+G(d) and B3LYP/6-311++G(d,p) Levels Including ZPVE Corrections[a]

	B3LYP/6-31+G(d)		B3LYP/6-311++G(d,p)	
	E + ZPVE	ΔE_0	E + ZPVE	ΔE_0
Cu^+ + 2-propanol	−1834.274437	53.4	−1834.494048	51.0
1	−1834.359609	0.0	−1834.575309	0.0
2	−1834.396537	−23.2	−1834.616777	−26.0
3	−1834.304338	34.7	−1834.518860	35.4
4	−1834.306479	33.3	−1834.519484	35.0
5	−1834.294627	40.8	−1834.508762	41.8
6	−1834.329460	18.9	−1834.545463	18.7
7	−1834.378930	−12.1	−1834.594234	−11.9
8	−1834.334534	15.7	−1834.555665	12.3
9	−1834.247047	70.6	−1834.453721[b]	76.3[b]
10	−1834.309050	31.7	−1834.522098	33.4
11	−1834.363874	−2.7	−1834.581901	−4.1
TS1-2	−1834.309794	31.3	−1834.526764	30.5
TS1-3	−1834.292838	41.9	−1834.508709	41.8
TS3-2	−1834.275076	53.0	−1834.489706	53.7
TS1-4	−1834.300162	37.3	−1834.515468	37.6
TS4-5	−1834.291040	43.0	−1834.504532	44.4
TS5-6	−1834.292933	41.8	−1834.505108[b]	44.1[b]
TS6-7	−1834.323343	22.8	−1834.541280	21.4
TS5-8	−1834.293465	41.5	−1834.512840	41.5
TS8-7	−1834.267882	57.6	−1834.488449	54.5
TS1-7	−1834.251610	67.8	−1834.470657	65.7
TS1-9	−1834.246158	71.2	−1834.454762	75.6
TS1-10	−1834.288818	44.4	−1834.504117	44.7
TS10-11	−1834.262567	60.9	−1834.478955	60.5
Cu^+−H_2O + propene	−1834.320715	24.4	−1834.544530	19.3
Cu^+−propene + H_2O	−1834.336784	14.3	−1834.559800	9.7
Cu^+−acetone + H_2	−1834.354225	3.4	−1834.566724	5.4
Cu^+−H_2 + acetone	−1834.287562	45.2	−1834.506499	43.2
Cu^+−2-propenol + H_2	−1834.309405	31.5	−1834.528077	29.6
Cu^+−H_2 + 2-propenol	−1834.261009	61.9	−1834.485699	56.2
Cu^+−ethenol + CH_4	−1834.337810	13.7	−1834.554846	12.8
Cu^+−CH_4 + ethenol	−1834.288226	44.8	−1834.511102	40.3
Me_2COH^+ + CuH	−1834.298915	38.1	−1834.513214	39.0

[a] Refer to Figures 1−5 for the notations of species. [b] Single-point calculation at B3LYP/6-311++G(d,p)//B3LYP/6-31+G(d).

at B3LYP/6-31+G(d) level, with the activation barrier of only 1.0 kcal/mol; however, we were not able to locate the TS at the B3LYP/6-311++G(d,p) level. Single-point B3LYP/6-311++G(d,p)//B3LYP/6-31+G(d) computation shows that **TS5-6** is 2.3 kcal/mol above **5**. Complex **6** can be viewed as the [Cu−H + Me_2COH^+] complex. It may dissociate to produce CuH + Me_2COH^+, or it may convert to species **7** via **TS6-7**. Species **7** dissociates to Cu^+−acetone + H_2 with 17.3 kcal/mol of energy. The overall barrier of the dehydrogenation with respect to **1** is 44.4 kcal/mol. In contrast, the barrier of dehydrogenation of free 2-propanol in the gas phase is predicted to be 80.1 kcal/mol at the B3LYP/6-311++G(d,p) level. The H_2 elimination reaction could take an alternative turn after intermediate **5** (path IV, Figure 3). The 1,4-H shift via **TS5-8** leads the reaction into **8**, the H_2−Cu^+−propenol complex that lies 12.3 kcal/mol on the PES. Complex **8** can rearrange into its keto form (complex **7**, see Figure 2); however, through a barrier that is higher in energy than the reactants, the complex can also dissociate into Cu^+−propenol + H_2 (29.6 kcal/mol) or Cu^+−H_2 + propenol (57.9 kcal/mol).

The direct, electrophile-assisted H_2 elimination (path V, Figure 4) has a high-energy barrier of 65.7 kcal/mol. It is evident that in path V the catalytic effect of copper cation is not as efficient as it is in the electrophile-assisted syn elimination of H_2O. This difference in catalytic ability of Cu^+ may be attributed to the fact that the copper cation does not activate the C_2−H bond as it does to the C_2−O bond in complex **1**.

The TSs and intermediates of O−H (path VI)-inserted Cu^+ complexes are shown in Figure 4. It is seen that the reaction path requires extra energy from the reactants; thus, the reactions are not likely to occur. In addition, the O−H insertion intermediate lies only on a shallow minimum on PES. We were unable to locate intermediate **9** at the B3LYP/6-311++G(d,p) level. A single-point B3LYP/6-31++G(d,p)// B3LYP/6-31+G(d) calculation shows that **9** is 0.7 kcal/mol above **TS1-9**. Complex **9** is thus barely a viable species.

Mechanisms involving O−H insertions of transition metal cations with alcohols were proposed by Jones and Staley.[39] However, the mechanism was not supported by the experiment of Weil and Wilkins.[22] The O−H-inserted intermediate, i.e., CH_4, was not observed in the experiments of Wilkins et al.[22] or Yeh et al.[1]

Finally, the reaction mechanism that involves C−C insertion of Cu^+ was studied. The TS connecting **1** and the C−C insertion complex (**10**) lies 44.7 kcal/mol on the PES. The relative energy of **10** is close to that of **4** (35.0 kcal/mol), the C−H insertion complex. However, the TS that leads to C−H insertion has a smaller barrier (**TS1-4**, 37.6 kcal/mol) than that of C−C insertion. In this case, the C−H bond is more easily activated by Cu^+ than the C−C bond. Further reaction of the C−C insertion channel results in CH_4 elimination and forms CH_4−Cu^+−ethenol complex (**11**). However, the reaction barrier is 9.5 kcal/mol above the reactants, despite the fact that its dissociation products (CH_4 + Cu^+−ethenol) are energetically accessible.

The C−C insertion mechnism (path VII) is also unlikely accroding to our predicted PES. The C−C-inserted intermediate **10** is lower in energy than the reactants; however, the TS (**TS10-11**) leading to the CH_4−Cu^+−ethenol complex (**11**) is higher in energy than the reactants. In the theoretical study of Siegbahn and Blomberg,[40] it was shown that in the oxidative additions of neutral (second row) transition metals and alkanes, the C−C bond is more difficult to activate than the C−H bond. Our study on the Cu^+ + 2-propanol reaction results in a similar conclusion. It can be seen in Figures 1 and 2 that our predicted PESs and the relative energies of products are in accord with the mechanisms proposed by the Wilkins et al. based on LD/FTMS measurements.[22]

Mass spectra for the reactions of deuterium-substituted 2-propanol would provide valuable information on the chemistry of Cu^+−2-propanol.[1] In the recent experiments performed by Yeh et al., mass spectra out of laser vaporization combined with supersonic molecular beam were reported for the Cu^+ ion reactions with $CH_3CH(OD)CH_3$ and with $CH_3CD(OH)CH_3$. According to our theoretical predictions, the following product channels are active in the experiment (in addition to complex **1**, in the order of relative energies of products).

For Cu^+ and $CH_3CH(OD)CH_3$,

$$Cu^+ + CH_3CH(OD)CH_3 \rightarrow HD + Cu^+{-}CH_3COCH_3 \quad (1, \text{III})$$

$$Cu^+ + CH_3CH(OD)CH_3 \rightarrow HDO + Cu^+{-}C_3H_6 \quad (2, \text{I})$$

$$Cu^+ + CH_3CH(OD)CH_3 \rightarrow C_3H_6 + Cu^+{-}HDO \quad (3, \text{I})$$

$$Cu^+ + CH_3CH(OD)CH_3 \rightarrow H_2 + Cu^+{-}CH_3C(OD){=}CH_2 \quad (4, \text{IV})$$

$$Cu^+ + CH_3CH(OD)CH_3 \rightarrow CuH + CH_3C(OD)CH_3^+ \quad (5, \text{III})$$

TABLE 4: Predicted Binding Energies (D_e, in kcal/mol) of Cu^+-L (L = Propene, H_2O, H_2, Acetone, 2-Propenol, CH_4, and Ethenol); D_0 Is Summarized in Parentheses

L	B3LYP/6-31+G(d)	B3LYP/6-311++G(d,p)
propene	54.0 (52.9)	50.9 (49.8)
H_2O	44.3 (42.8)	41.9 (40.2)
H_2	16.0 (14.3)	17.6 (15.7)
acetone	57.5 (56.1)	54.4 (53.4)
2-propenol	45.0 (44.7)	42.7 (42.2)
CH_4	22.2 (22.1)	22.6 (22.3)
ethenol	54.7 (53.2)	51.1 (49.7)

and for Cu^+ and $CH_3CD(OH)CH_3$,

$$Cu^+ + CH_3CD(OH)CH_3 \rightarrow HD + Cu^+-CH_3COCH_3 \quad (6, III)$$

$$Cu^+ + CH_3CD(OH)CH_3 \rightarrow H_2O + Cu^+-CH_2CDCH_3 \quad (7, I)$$

$$Cu^+ + CH_3CD(OH)CH_3 \rightarrow CH_2CDCH_3 + Cu^+-H_2O \quad (8, I)$$

$$Cu^+ + CH_3CD(OH)CH_3 \rightarrow HD + Cu^+-CH_3C(OH)=CH_2 \quad (9, IV)$$

$$Cu^+ + CH_3CD(OH)CH_3 \rightarrow CuD + CH_3C(OH)CH_3^+ \quad (10, III)$$

The fragmentation product distributions 1−3 and 6−8 were exclusively identified in the mass spectra of Yeh et al. In contrast, channels 4, 5 and 9, 10 have not been located by the apparatus. The result can be attributed to the relative abundances of species. However, it has to be noted that unlike the experiment of Wilkins et al.,[22] the reactions of Yeh et al.[1] do not occur under thermal conditions. Overall, our predicted PESs are consistent with the experiments.

The Cu^+-ligand binding energies are summarized in Table 4. Among all organic compounds studied, Cu^+ cation binds most strongly to acetone (53.4 kcal/mol). The bindings of Cu^+ with propene and ethenol are also strong. The large binding energy to ethenol, however, is attributed to the unstable compound ethenol. The binding energies of Cu^+ with CH_4 and H_2 are significantly smaller.

4. Conclusions

The reaction paths on the Cu^+-2-propanol PES have been explored using DFT. The binding energy for Cu^+ with 2-propanol has been predicted to be 51.0 kcal/mol, which is about 10 kcal/mol larger than that of Cu^+-H_2O. The overall minimum energy path is the syn elimination of H_2O (30.5 kcal/mol, path I). Another H_2O elimination pathway experiences a higher energy barrier (path II); however, the energy is still comparable to the energy of the reactants Cu^+ + 2-propanol. The energy barrier of dehydrogenation via C−H insertion (paths III, IV) is 44.4 kcal/mol on PES. Direct H_2 elimination, where Cu^+ acts as a bystander (path V), was found to be energetically unfavorable. The O−H insertion channel (path VI) was shown to be also unlikely. We have also found that it is more difficult to activate the C−C bond than the C−H bond. The C−C insertion mechanism involves a TS that is higher in energy than the reactants. Among all active channels, the relative energies of the fragment products are $[Cu-acetone^+ + H_2] < [Cu-propene^+ + H_2O] < [Cu^+-H_2O + propene] < [Cu^+-2\text{-}propenol + H_2] < [CuH + Me_2COH^+]$; the results are consistent with available gas phase experiments.

Acknowledgment. This work was supported by the National Science Council of Taiwan, Republic of China. We thank the National Center for High-Performance Computing for computer time and facilities.

References and Notes

(1) Huang, Y.-C.; Su, P.-H.; Yeh, C.-S. *Bull. Chem. Soc. Jpn.* **2001**, *74*, 677.
(2) Nakao, Y.; Taketsugu, T.; Hirao, K. *J. Chem. Phys.* **1999**, *110*, 10863.
(3) Alcamí, M.; Mó, O.; Yáñez, M.; Luna, A.; Morizur, J. P.; Tortajada, J. *J. Phys. Chem. A* **1998**, *102*, 10120.
(4) Luna, A.; Amekraz, B.; Morizur, J. P.; Tortajada, J.; Mó, O.; Yáñez, M. *J. Phys. Chem. A* **2000**, *104*, 3132.
(5) Luna, A.; Morizur, J. P.; Tortajada, J.; Alcamí, M.; Mó, O.; Yáñez, M. *J. Phys. Chem. A* **1998**, *102*, 4652.
(6) Stöckigt, D. *J. Phys. Chem. A* **1998**, *102*, 10493.
(7) Luna, A.; Gevrey, S.; Tortajada, J. *J. Phys. Chem. B* **2000**, *104*, 110.
(8) Russo, N.; Sicilia, E. *J. Am. Chem. Soc.* **2001**, *123*, 2588.
(9) Luna, A.; Amekraz, B.; Morizur, J. P.; Tortajada, J.; Mó, O.; Yáñez, M. *J. Phys. Chem. A* **1997**, *101*, 5931.
(10) Guo, J.; Goodings, J. M. *Chem. Phys. Lett.* **2001**, *342*, 169.
(11) Luna, A.; Amekraz, B.; Tortajada, J. *Chem. Phys. Lett.* **1997**, *226*, 31.
(12) Irigoras, A.; Elizalde, O.; Silanes, I.; Fowler, J. E.; Ugalde, J. M. *J. Am. Chem. Soc.* **2000**, *122*, 114.
(13) Irigoras, A.; Fowler, J. E.; Ugalde, J. M. *J. Phys. Chem. A* **1998**, *102*, 293.
(14) Luna, A.; Amekraz, B.; Morizur, J. P.; Tortajada, J.; Mó, O.; Yáñez, M. *J. Phys. Chem. A* **1997**, *101*, 5931.
(15) Luna, A.; Amekraz, B.; Tortajada, J.; Morizur, J. P.; Alcami, M.; Mó, O.; Yáñez, M. *J. Am. Chem. Soc.* **1998**, *120*, 5411.
(16) Nakao, Y.; Taketsugu, T.; Hirao, K. *J. Chem. Phys.* **1999**, *110*, 10863.
(17) Bouchards, F.; Brenner, V.; Carra, C.; Hepburn, J. W.; Koyanagi, G. K.; McMahon, T. B.; Ohanessian, G.; Peschke, M. *J. Phys. Chem. A* **1997**, *101*, 5885.
(18) Zhang, X.-G.; Liyanage, R.; Armentrout, P. B. *J. Am. Chem. Soc.* **2001**, *123*, 5563.
(19) Boutreau, L.; Leon, E.; Luna, A.; Toulhoat, P.; Tortajada, J. *Chem. Phys. Lett.* **2001**, *338*, 74.
(20) Russo, N.; Sicilla, E. *J. Am. Chem. Soc.* **2001**, *123*, 2588.
(21) Jones, R. W.; Staley, R. H. *J. Phys. Chem.* **1982**, *86*, 1669.
(22) Weil, D. A.; Wilkins, C. L. *J. Am. Chem. Soc.* **1985**, *107*, 7316.
(23) Frisch, M. J.; Trucks, G. W.; Schlegel, H. B.; Scuseria, G. E.; Robb, M. A.; Cheeseman, J. R.; Zakrzewski, V. G.; Montgomery, J. A., Jr.; Stratmann, R. E.; Burant, J. C.; Dapprich, S.; Millam, J. M.; Daniels, A. D.; Kudin, K. N.; Strain, M. C.; Farkas, O.; Tomasi, J.; Barone, V.; Cossi, M.; Cammi, R.; Mennucci, B.; Pomelli, C.; Adamo, C.; Clifford, S.; Ochterski, J.; Petersson, G. A.; Ayala, P. Y.; Cui, Q.; Morokuma, K.; Malick, D. K.; Rabuck, A. D.; Raghavachari, K.; Foresman, J. B.; Cioslowski, J.; Ortiz, J. V.; Stefanov, B. B.; Liu, G.; Liashenko, A.; Piskorz, P.; Komaromi, I.; Gomperts, R.; Martin, R. L.; Fox, D. J.; Keith, T.; Al-Laham, M. A.; Peng, C. Y.; Nanayakkara, A.; Gonzalez, C.; Challacombe, M.; Gill, P. M. W.; Johnson, B.; Chen, W.; Wong, M. W.; Andres, J. L.; Gonzalez, C.; Head-Gordon, M.; Replogle, E. S.; Pople, J. A. *Gaussian 98*, Revision A.3; Gaussian, Inc.: Pittsburgh, PA, 1998.
(24) Becke, A. D. *J. Chem. Phys.* **1993**, *98*, 5648.
(25) Lee, C.; Yang, W.; Parr, R. G. *Phys. Rev. B* **1988**, *37*, 785.
(26) Salter, E. A.; Trucks, G. W.; Bartlett, R. J. *J. Chem. Phys.* **1989**, *90*, 1752.
(27) Scuseria, G. E.; Schaefer, H. F., III. *J. Chem. Phys.* **1989**, *90*, 3700.
(28) Boys, S. F.; Bernardi, F. *Mol. Phys.* **1970**, *19*, 553.
(29) González, C.; Schlegel, H. B. *J. Phys. Chem.* **1989**, *90*, 2154.
(30) Bauschlicher, C. W.; Langhoff, S. R.; Partridge, H. *J. Chem. Phys.* **1991**, *94*, 2068.
(31) Schneider, W. F.; Hass, K. C.; Ramprasad, R.; Adams, J. B. *J. Chem. Phys.* **1996**, *100*, 6032.
(32) Hoyau, S.; Ohanessian, G. J. *Chem. Phys. Lett.* **1997**, *266*, 31.
(33) El-Nahas, A. M.; Tajima, N.; Hirao, K. *J. Mol. Struct. (THEOCHEM)* **1999**, *469*, 201.
(34) El-Nahas, A. M.; Hirao, K. *J. Phys. Chem. A* **2000**, *104*, 138.

(35) Magnera, T. F.; David, D. E.; Stulik, D.; Orth, R. G.; Jonkman, H. T.; Michl, J. *J. Am. Chem. Soc.* **1989**, *111*, 5036.

(36) Armentrout, P. B.; Kickel, B. L. In *Organometallic Ion Chemistry*; Freiser, B. S., Ed.; Kluwer Academic Publishers: Norewell, MA, 1996; p 1.

(37) Rassolov, V.; Pople, J. A.; Ratner, M.; Windus, T. L. *J. Chem. Phys.* **1998**, *109*, 1223.

(38) (a) Wachters, A. J. H. *J. Chem. Phys.* **1970**, *52*, 1033. (b) Hay, P. J. *J. Chem. Phys.* **1997**, *66*, 4377.

(39) Huang, S.; Holman, R. W.; Gross, M. L. *Organometallics* **1986**, *5*, 1857.

(40) Siegbahn, P. E. M.; Blomberg, M. R. A. In *Theoretical Aspects of Homogeneous Catalysis*; van Leeuwen, P. W. N. M., Morokuma, K., van Lenthe, J. H., Eds.; Kluwer Academic Publishers: The Netherlands, 1995.